

# Fully automatic differential diagnosis system for dementia with Lewy bodies and Alzheimer's disease using FDG-PET and 3D-SSP

Atsushi K. Kono · Kazunari Ishii · Keitaro Sofue ·  
Naokazu Miyamoto · Setsu Sakamoto · Etsuro Mori

Received: 25 October 2006 / Accepted: 24 January 2007 / Published online: 22 February 2007  
© Springer-Verlag 2007

## Abstract

**Purpose** To evaluate a fully automatic computer-assisted diagnostic system for mild dementia with Lewy bodies (DLB), permitting distinction from mild Alzheimer's disease (AD).

**Methods** Using  $^{18}\text{F}$ -fluorodeoxyglucose and positron emission tomography (FDG-PET), glucose metabolic images were obtained from mild DLB and mild AD patients. Two groups consisting of 16 mild DLB patients and 21 mild AD patients were recruited for diagnostic evaluation between mild DLB and mild AD. The mean age  $\pm$  SD of the mild DLB group and the mild AD group was  $74.3 \pm 4.9$  and  $71.7 \pm 2.1$  years, respectively, and the mean scores of the MMSE for the mild DLB and the mild AD group were  $21.7 \pm 1.9$  and  $23.1 \pm 2.1$ , respectively. A receiver operating characteristic (ROC) analysis was performed to compare the diagnostic performance, in terms of discrimination between DLB and AD, of conventional axial FDG-PET images inspected visually by experts and beginners with that of our fully automatic diagnosis system using the statistical brain mapping method and Z scores obtained with the DLB template.

**Results** The diagnostic performance of the automatic system was comparable to that of visual inspection by experts. The area under the ROC curve for the automatic diagnosis system was 0.77. The mean area under the ROC curve for visual inspection by experts and beginners was 0.76 and 0.65, respectively.

**Conclusion** The fully automatic differential diagnosis system for distinction between mild DLB and AD showed a similar diagnostic accuracy to visual inspection by experts. It would be a useful diagnostic tool to distinguish mild DLB from mild AD in clinical practice.

**Keywords** Dementia with Lewy bodies · Cerebral glucose metabolism · Fluorodeoxyglucose · Positron emission tomography · Computer-assisted diagnosis

## Introduction

Dementia with Lewy bodies (DLB) is a degenerative dementia that is pathologically characterized by the development of abnormal  $\alpha$ -synuclein cytoplasmic inclusions, called Lewy bodies, throughout the brain in cortical, subcortical and brainstem structures. As the number of patients with dementia has increased, so the number of patients with DLB, the second most frequent cause of degenerative dementia in elderly adults, has also increased. DLB is estimated to account for about 20% of cases of dementia [1, 2]. In 1996, a consortium of scientists initially proposed guidelines for the clinical and pathological diagnosis of dementia with Lewy bodies [3]; these were later revised [4], and the guidelines have been gradually adopted in clinical practice. Central features of DLB include progressive cognitive decline and include recurrent visual hallucinations, fluctuating cognition and parkinsonism. Functional

---

A. K. Kono · K. Ishii (✉) · K. Sofue · N. Miyamoto  
Department of Radiology and Nuclear Medicine,  
Hyogo Brain and Heart Center,  
520 Saisho-Ko,  
Himeji, Hyogo 670-0981, Japan  
e-mail: kishii@hbhc.jp

S. Sakamoto  
PET Center, Himeji Central Hospital,  
Himeji, Hyogo, Japan

E. Mori  
Behavioral Neurology and Cognitive Neuroscience, Tohoku  
University Graduate School of Medicine,  
Sendai, Miyagi, Japan

brain images support its diagnosis by demonstrating occipital metabolic or perfusion reduction in addition to the parietotemporal and posterior cingulate metabolic and perfusion reduction which is observed in Alzheimer's disease (AD). From a prognostic and therapeutic standpoint, it is important to discriminate DLB patients from AD patients because the former have a favourable response to cholinesterase inhibitors and symptomatic treatments, and the treatment for the two diseases is not the same owing to their differing pathogenesis.

Recently, we developed a fully automatic diagnosis system for early AD [5] using the NEUROSTAT program [6]. As the next step, in this study we developed this into a fully automatic diagnosis system for differentiation between DLB and AD. We evaluated the differential diagnostic value compared with conventional inspection of FDG-PET images in mild DLB and mild AD patients.

## Materials and methods

### Subjects and PET procedure

The concept of this method is based on our previous method [5]. In order to establish an appropriate prototype ROI template for differentiating DLB from AD patients, first ten patients with mild DLB and 20 patients with mild AD were recruited. The AD group consisted of the subjects used for the previous fully automatic system for AD diagnosis [5]. The mean age  $\pm$  standard deviation (SD) of the mild DLB group and the AD group was  $71.2 \pm 4.3$  and  $70.9 \pm 2.7$  years, respectively (Table 1, "first group"). Two further groups consisting of 16 mild DLB patients and 25 mild AD patients were recruited for diagnostic evaluation between DLB and AD using this method. The mean age  $\pm$  SD of the mild DLB group and the mild AD group were  $74.3 \pm 4.9$  and  $71.7 \pm 2.1$ , respectively (Table 1, "second group"). The mean scores of the MMSE for DLB and AD in the first group and for DLB and AD in the second group were  $23.0 \pm 3.2$ ,  $22.8 \pm 1.5$ ,  $21.7 \pm 1.9$  and  $23.1 \pm 2.1$ , respectively (Table 1). Both groups of DLB patients fulfilled the

criteria of the First International Workshop of the Consortium on Dementia with Lewy Bodies [3]. Both groups of AD patients fulfilled the NINCDS/ADRDA criteria for probable AD [7]. All patients were examined by both neuropsychologists and psychiatrists. Electroencephalography, laboratory tests and neuropsychological tests, MRI and MR angiography of the neck and head were also performed.

The MR imaging and PET scanning methods are described in detail elsewhere [8]. In all patients, MR examinations for diagnosis were performed before PET scanning. All subjects fasted for 4 h before PET. After a transmission scan, a 12-min emission scan was started 60 min after intravenous injection of 185–296 MBq of FDG. PET images were obtained using a Headtome IV scanner (Shimadzu Corp., Kyoto, Japan). Data were collected in  $128 \times 128$  matrices. The slice interval was 6.5 mm when the z-motion mode was used. Written informed consent was obtained from all subjects before the examination.

### Automatic diagnosis system procedure

#### 1. Creation of a prototype ROI map

First, stereotactic anatomical standardization was performed. The original FDG-PET image data were transformed into a binary format. They were transformed into a standard Talairach space using the NEUROSTAT program [6], which contains all three-dimensional stereotactic surface projection (3D-SSP) programs (Dr. Minoshima, Department of Radiology and Bioengineering, University of Washington, Seattle, USA). Differences in size between the individual brain and the standard template were removed by linear scaling. Regional anatomical differences between the individual and the standard template were minimized by automated non-linear warping. Next, peak cortical activity in the brain was subjected to a three-dimensional search with a predefined vector for each stereotactic surface pixel after anatomical standardization. The peak value was projected back and assigned to the originating surface pixel. This procedure was continued on a pixel-by-pixel basis covering the whole cortex of the brain. Pixel values of an individual's image set were normalized to the whole brain, the thalamus, the pons, the cerebellum and the sensorimotor value with the 3D-SSP program in NEUROSTAT [6]. The sensorimotor cortices were defined as reference regions for normalization [9, 10]. Pixels with significantly decreased metabolism in the DLB group ( $p < 0.05$ ), which were obtained from a comparison between the AD group and the DLB group (the first group), were plotted as a prototype DLB ROI map (Fig. 1). The AD group had no regions with significantly lower metabolism compared with the DLB group (the first group).

**Table 1** Patient characteristics: number, age and MMSE score

		No.	Age (yrs)	MMSE
First group	DLB	10	$71.2 \pm 4.3$	$23.0 \pm 3.2$
	AD	20	$70.9 \pm 2.7$	$22.8 \pm 1.5$
Second group	DLB	16	$74.3 \pm 4.9$	$21.7 \pm 1.9$
	AD	25	$71.7 \pm 2.1$	$23.1 \pm 2.1$

All values except number of subjects are presented as mean  $\pm$  standard deviation

DLB dementia with Lewy Bodies, AD Alzheimer's disease, MMSE Mini-mental State Examination score.

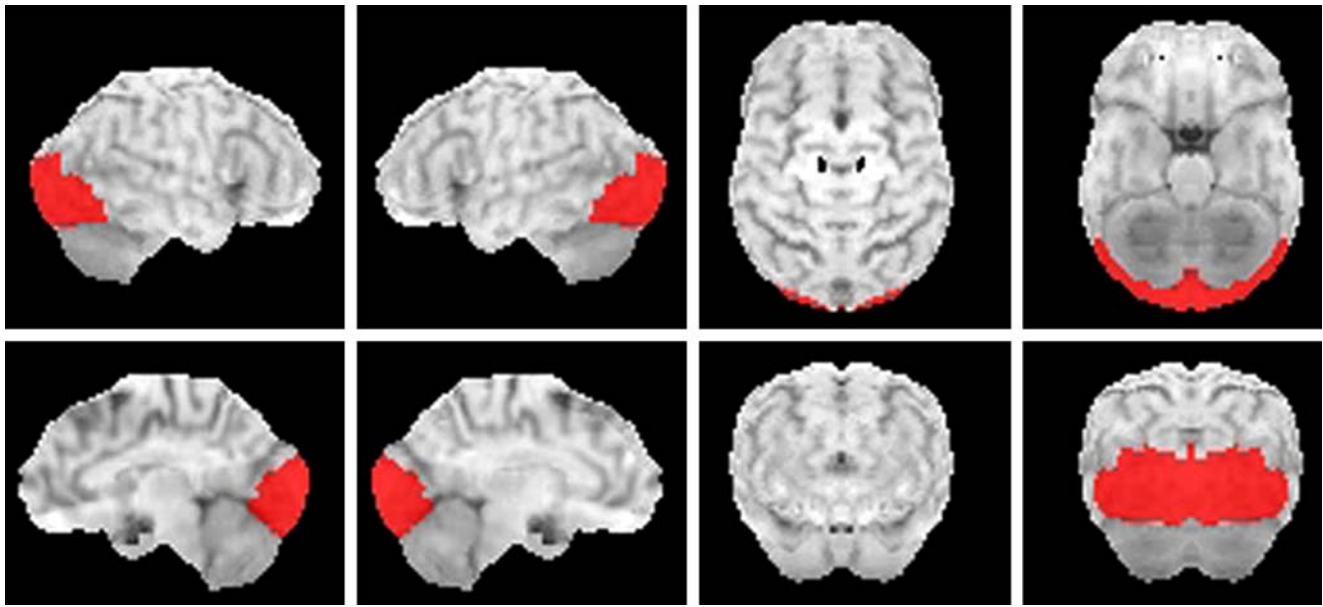


**Fig. 1** Prototype ROI map for mild DLB, which demonstrates significantly lower metabolism in DLB than in AD. The automatic diagnosis system uses this ROI map

## 2. Acquisition of threshold Z scores in the prototype ROI maps for diagnosis.

For each individual surface projection image, a Z score was calculated for each pixel— $Z \text{ score} = \frac{[\text{normal mean}] - [\text{individual value}]}{(\text{normal SD})}$ —using a normal database produced in the previous study [5], and the scores were shown as a Z score map. The averaged Z scores in each area of the prototype DLB ROI map were calculated. Two threshold values were tested, mean+2SD and mean+3SD, these values being derived from the AD patients in the first group. The mean and SD and threshold values in each region of the first group are shown in Table 2.

## 3. Clinical adoption of the system.

In the same way, the Z score images of the second group were obtained and the averaged Z scores were also calculated with the ROI map. We diagnosed as DLB any subject with more than one area in the bilateral medial and lateral occipital lobes where averaged Z scores exceeded the thresholds for DLB in this system.

## Comparison of the diagnostic performance of conventional FDG-PET imaging and the fully automatic method

We compared the diagnostic performance of visual inspection with that of the automatic method. Each image of the second group was displayed on a colour monitor. Five observers, three experienced and two beginners, reviewed the conventional FDG-PET images. All of them knew the criteria for abnormality but were blinded to the patients' clinical data. The conventional FDG-PET images were classified as follows: (1) definite DLB, (2) probable DLB, (3) indeterminate, (4) probable AD or (5) definite AD. In the automatic method, each patient's average for each region was obtained in reference to the prototype DLB map, and the diagnosis of DLB was made if the averaged Z score exceeded the determined value.

We performed a receiver operating characteristic (ROC) analysis to compare the automatic system with visual reading. For ROC analysis of the fully automatic diagnosis

**Table 2** The averaged Z scores in each area of the prototype DLB ROI map calculated in the first group, and obtained thresholds

	Right lateral occipital		Left lateral occipital		Right medial occipital		Left medial occipital	
	Mean	(SD)	Mean	(SD)	Mean	(SD)	Mean	(SD)
DLB	927	(429)	766	(331)	227	(174)	192	(160)
AD	235	(177)	261	(256)	83	(73)	71	(59)
Threshold	A	588	A	773	A	230	A	188
	B	765	B	1,029	B	303	B	247

DLB dementia with Lewy bodies, AD Alzheimer's disease, SD standard deviation, threshold A mean+2SD of the first group, threshold B mean+3SD of the first group

**Table 3** The averaged Z scores in each area of the prototype DLB ROI map calculated in the second group

	Right lateral occipital		Left lateral occipital		Right medial occipital		Left medial occipital	
	Mean	(SD)	Mean	(SD)	Mean	(SD)	Mean	(SD)
DLB	758	(363)	709	(290)	224	(111)	211	(126)
AD	235	(177)	261	(256)	83	(73)	71	(59)

Abbreviations as in Table 2

system, the averaged Z scores in the prototype ROI map of each subject in the second group were used. The areas under the curves were calculated using ROCKIT software 0.9B (Dr. Metz, Department of Radiology, The University of Chicago).

## Results

The averaged Z scores in each area of the ROI map obtained in the second group are shown in Table 3. All the averaged Z scores in each region for DLB were significantly larger than those for AD. The fully automatic diagnosis system demonstrated an accuracy of 73%, a sensitivity of 75% and a specificity of 72% for the mild DLB group when the threshold was set at the mean+2SD. When using the threshold of the mean+3SD, an accuracy of 61%, a sensitivity of 38% and a specificity of 76% were demonstrated.

Figure 2 shows each observer's area under the ROC curve ( $A_z$ ) for visual inspection of conventional FDG-PET images ( $A_z=0.83-0.58$ ) and for the fully automatic diagnosis system ( $A_z=0.77$ ), using the threshold of mean+2SD. There was no significant difference in the area under the ROC curve between the automatic diagnosis system and the visual inspections. The diagnostic value of the automatic system was compared with that of the observers (Table 4).

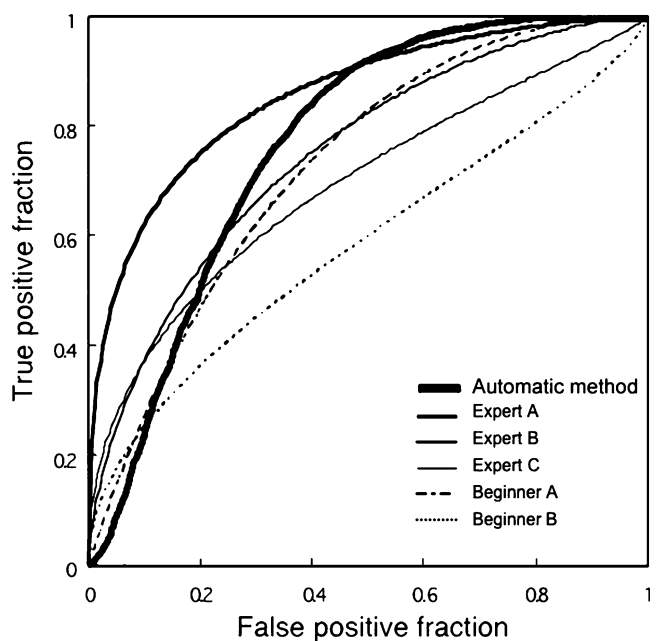
### Representative cases

Figure 3 shows the conventional FDG-PET images (a) and Z score map (b) of a 74-year-old male patient with DLB. His MMSE score was 26. All the observers could easily diagnose this case as DLB by visual inspection of the conventional FDG-PET images because of a typical metabolic reduction pattern. The automatic diagnosis system also diagnosed it as DLB. Figure 4 shows the conventional FDG-PET images (a) and Z score map (b) of a 71-year-old female with AD. All the observers and the automatic system could diagnose this case as AD. Figure 5 shows the findings in a 74-year-old male DLB patient with an MMSE score of 21; two experts and one beginner diagnosed this case as DLB, while the other expert

considered it equivocal and the other beginner diagnosed it as AD. The automatic diagnosis system could not diagnose this case as DLB.

## Discussion

The First International Workshop of the Consortium on Dementia with Lewy Bodies drew up guidelines for the clinical and pathologic diagnosis of DLB in 1996 [3]. Since that publication, a number of reports in the literature have concluded that the criteria have low sensitivity and high specificity. Several factors, such as poor reliability of fluctuating cognition and the lack of parkinsonism and visual hallucinations, probably contribute to the low sensitivity [3, 11–15]. A sensitivity of 75% and a specificity of 79% were documented in a preliminary validation study of the criteria [11], and a new validation study using the revised criteria [4] is needed. The overlap between the



**Fig. 2** ROC curves for DLB patients versus AD patients obtained with visual inspection by experts or beginners or by use of the automatic diagnosis system. The area under the ROC curve of beginner B is significantly smaller than that of other observers

**Table 4** Area under ROC curves for the automatic diagnosis system and individual observers

	$A_z$	Accuracy (%)
Automatic diagnosis system	0.7712	70.0
Expert A	0.8323	76.7
Expert B	0.7446	67.3
Expert C	0.6908	63.0
Beginner A	0.7245	65.7
Beginner B	0.5803	55.3

$A_z$  area under the ROC curve

clinical symptoms and pathology of DLB with those of AD can lead to misdiagnosis. The low sensitivity of the aforementioned criteria indicates that DLB is likely to be misdiagnosed particularly at the early stage. It is very important to diagnose early DLB accurately and to distinguish it from other dementia diseases because the treatment and prognosis differ. We have previously reported an automatic system using 3D-SSP for the diagnosis of early AD [5]. In the present study, we assessed the usefulness of this system, which is independent of operator skill, in distinguishing mild DLB from mild AD.

Diagnostic imaging methods, such as MRI or nuclear medicine methods, are helpful in diagnosing DLB accurately. The revised consortium proposed that imaging investigation can also be helpful in supporting a diagnosis [4]. In DLB, the volume of the hippocampal and the medial temporal lobe is preserved and atrophy of the putamen is demonstrated by MRI volumetry. However, it is not easy to demonstrate the morphological difference between mild DLB and mild AD. Occipital hypoperfusion on single-

photon emission computed tomography (SPECT) and hypometabolism on PET have been shown without occipital lobe atrophy on MRI [16–19]. The metabolism and perfusion of the medial and lateral occipital lobe are characteristically affected in DLB, and these are the features that discriminate it from AD [20]. Dopaminergic and cholinergic impairment is considered to be the cause of the hypometabolism and hypoperfusion in the occipital lobe [3, 16, 21, 22]. In this study we tried to diagnose mild DLB with occipital hypometabolism using FDG-PET and 3D-SSP automatically. We used the NEUROSTAT program for 3D-SSP, which is able to transform atrophied brain to standard brain more correctly than the statistical parametric mapping (SPM) method [23] and to compensate for inappropriate anatomical standardization [6]. An important step in this statistical method was the selection of the reference area for the normalization: we chose the sensorimotor area for this system because of the relative preservation of metabolism in the sensorimotor cortex in DLB patients [10]. The fully automatic diagnosis system for differentiation of mild DLB from mild AD was able to perform at a similar diagnostic level to visual inspection of conventional axial FDG-PET images by expert readers.

As shown in our study, although visual inspection by the readers provided good diagnostic accuracy, the area under the ROC curve was not as large as we had expected (mean  $A_z=0.7145$ ). It can be difficult to make a diagnosis of mild DLB because occipital glucose metabolism is not always decreased more severely in mild DLB than in mild AD. The difference in the metabolic reduction between mild DLB and AD was smaller than we had anticipated, and this may be the reason why even experts had difficulty in diagnosing

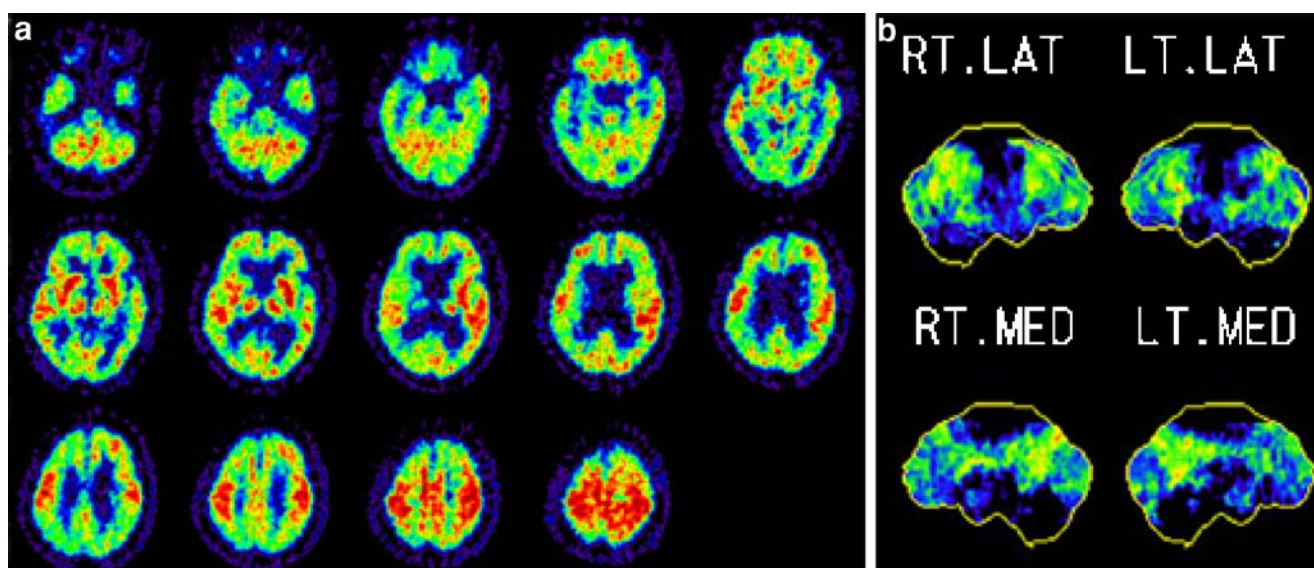


**Fig. 3** Conventional FDG PET images (a) and Z score images (b) of a 74-year-old patient with DLB (MMSE 26). It is easy to detect decreased glucose metabolism in the bilateral occipital lobe by visual inspection and to diagnose the case as DLB

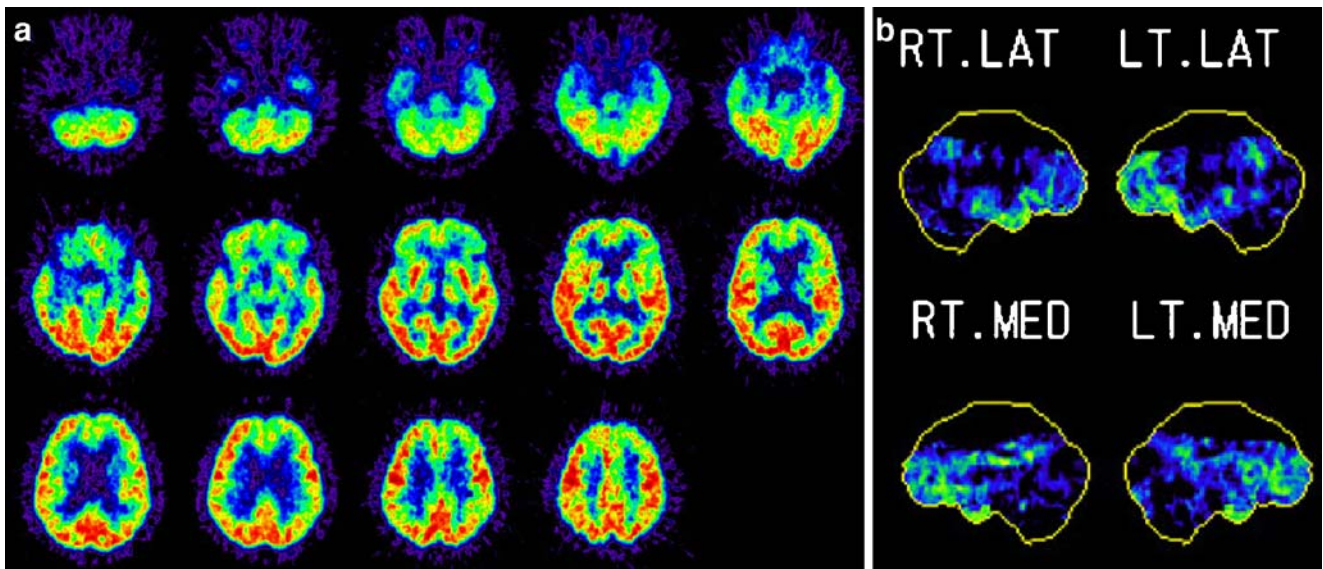


**Fig. 4** Conventional FDG PET images (a) and Z score images (b) of a 71-year-old patient with AD (MMSE 22). Decreased glucose metabolism in the bilateral frontal and parietotemporal association

cortices can be seen. All the readers and the automatic diagnosis system could diagnose this case as AD

some of the mild DLB cases in this study. The area under the ROC curve was accordingly small, and the same results were obtained using our automatic diagnosis system. It is also to be borne in mind that while DLB accounts for about 20% of dementia cases, in the sample in this study the percentage was 40%. Since DLB patients also show the patterns of AD on FDG-PET images, this high prevalence of DLB may have led to underestimation of the diagnostic performance of the readers and of the automatic method as well. While our diagnostic system performed similarly to

the experts in diagnosing mild DLB, the ROC curve of the automatic system was shifted slightly to the right; this indicates that the diagnostic performance in respect of AD patients varied more widely than that in respect of DLB patients (i.e. there were fewer misdiagnoses in DLB patients), and in clinical use this system might have the advantage of having a high sensitivity for identification of early DLB.

Neuroimaging for assessment of nigrostriatal dopaminergic function is also useful [24]. In DLB there is a 40–70%

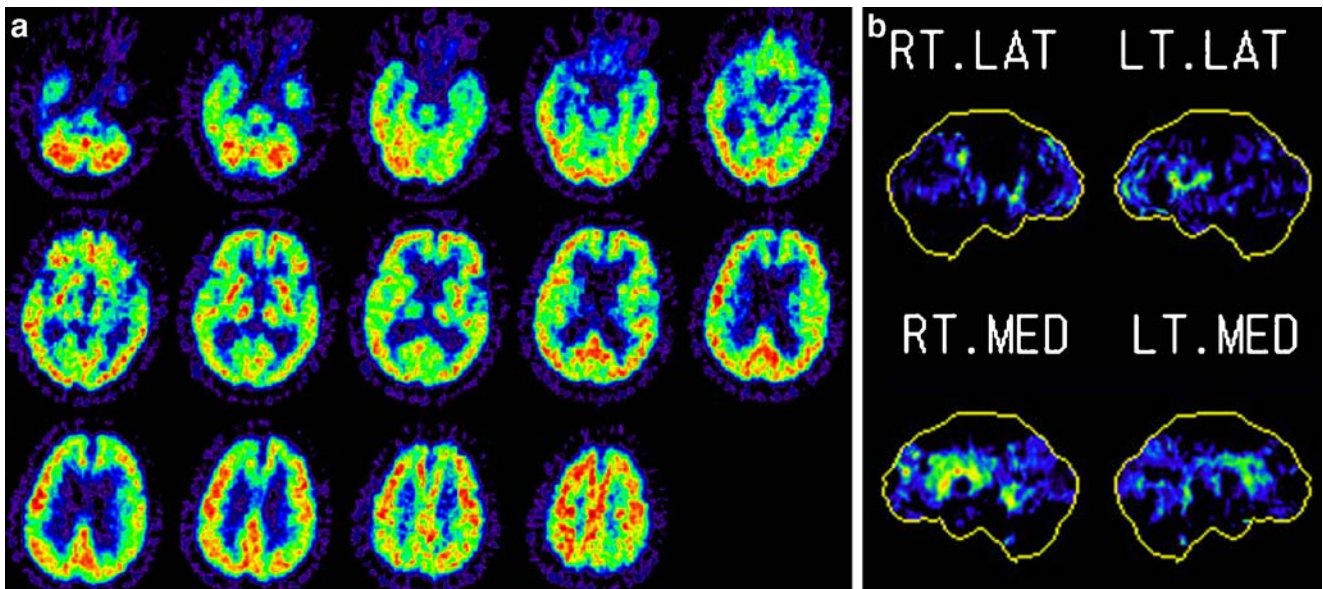


**Fig. 5** Conventional FDG PET images (a) and Z score images (b) of a 74-year-old patient with DLB (MMSE 21). Heterogeneously decreased glucose metabolism can be seen. The Z score image failed to demonstrate significant reduction

loss of striatal dopamine, and the loss of dopaminergic cells is accompanied by dopamine transporter loss [25]. Ligand imaging for the dopamine transporter provides a marker for presynaptic neuronal degeneration. When using  $^{123}\text{I}$ -radio-labelled  $2\beta$ -carbomethoxy- $3\beta$ -(4-iodophenyl)- $N$ -(3-fluoropropyl) nortropine ( $^{123}\text{I}$ -FP-CIT) SPECT, areas under the ROC curves were greater than 0.92, demonstrating good power in discriminating between DLB and AD [26]. Demonstration of reduction in the uptake of  $^{18}\text{F}$ -fluorodopa in the caudate and putamen using PET distinguishes between DLB and AD with high sensitivity and specificity [27]. On the other hand, FDG-PET is an accepted technique for the detection of AD, especially when the diagnosis is uncertain. Consequently we would suggest that the proposed automatic diagnosis system and FDG-PET could first be employed to investigate the possible presence of DLB in patients suspected of having AD, with the use of FP-CIT scan for further investigation when necessary. In future we are going to apply this method to SPECT perfusion studies which are more widely used than FDG-PET. Now that we have developed a fully automatic diagnosis system for AD and DLB, we also wish to expand this system to other degenerative dementias.

## Conclusion

We have developed a fully automatic diagnosis system that can be employed to distinguish mild DLB from mild AD using 3D-SSP. Its diagnostic value is considered to be comparable to expert reading of conventional FDG-PET images. This method could be applied to detect cases of mild DLB in routine clinical examinations.

**Acknowledgements** The authors thank Mr. Shuya Miki (Nihon Medi-Physics, Nishinomiya, Hyogo, Japan) for providing and improving the iSSP program which uses the 3D-SSP program and was dedicated to this automatic method.

## References

- Perry RH, Irving D, Blessed G, Perry EK, Fairbairn AF. Clinically and neuropathologically distinct form of dementia in the elderly. *Lancet* 1989;I:166.
- Perry RH, Irving D, Tomlinson BE. Lewy body prevalence in the aging brain: relationship to neuropsychiatric disorders, Alzheimer-type pathology and catecholaminergic nuclei. *J Neurol Sci* 1990;100:223–33.
- McKeith IG, Galasko D, Kosaka K, Perry EK, Dickson DW, Hansen LA, et al. Consensus guidelines for the clinical and pathologic diagnosis of dementia with Lewy bodies (DLB): report of the consortium on DLB international workshop. *Neurology* 1996;47:1113–24.
- McKeith IG, Dickson DW, Lowe J, Emre M, O'Brien JT, Feldman H, et al. Diagnosis and management of dementia with Lewy bodies: third report of the DLB Consortium. *Neurology* 2005;65:1863–72.
- Ishii K, Kono AK, Sasaki H, Miyamoto N, Fukuda T, Sakamoto S, et al. Fully automatic diagnostic system for early- and late-onset mild Alzheimer's disease using FDG PET and 3D-SSP. *Eur J Nucl Med Mol Imaging* 2006;33:575–83.
- Minoshima S, Frey KA, Koeppe RA, Foster NL, Kuhl DE. A diagnostic approach in Alzheimer's disease using three-dimensional stereotactic surface projections of fluorine-18-FDG PET. *J Nucl Med* 1995;36:1238–48.
- McKhann G, Drachman D, Folstein M, Katzman R, Price D, Stadlan E. Clinical diagnosis of Alzheimer's disease: report of the NINCDS-ADRDA Work Group under the auspices of Department of Health and Human Services Task Force on Alzheimer's Disease. *Neurology* 1984;34:939–44.
- Ishii K, Sasaki M, Kitagaki H, Yamaji S, Sakamoto S, Matsuda K, et al. Reduction of cerebellar glucose metabolism in advanced Alzheimer's disease. *J Nucl Med* 1997;38:925–8.
- Ishii K, Yamaji S, Mori E. Cerebellar metabolic reduction in Alzheimer's disease and data normalization. *J Nucl Med* 1998;39:375–6.
- Ishii K, Imamura T, Sasaki M, Yamaji S, Sakamoto S, Kitagaki H, et al. Regional cerebral glucose metabolism in dementia with Lewy bodies and Alzheimer's disease. *Neurology* 1998;51:125–30.
- Mega MS, Masterman DL, Benson DF, Vinters HV, Tomiyasu U, Craig AH, et al. Dementia with Lewy bodies: reliability and validity of clinical and pathologic criteria. *Neurology* 1996;47:1403–9.
- Litvan I, MacIntyre A, Goetz CG, Wenning GK, Jellinger K, Verny M, et al. Accuracy of the clinical diagnoses of Lewy body disease, Parkinson disease, and dementia with Lewy bodies. A clinicopathologic study. *Arch Neurol* 1998;55:969–78.
- Hohl U, Tiraboschi P, Hansen LA, Thal LJ, Corey-Bloom J. Diagnostic accuracy of dementia with Lewy bodies. *Arch Neurol* 2000;57:347–51.
- Lopez OL, Becker JT, Kaufer DJ, Hamilton RL, Sweet RA, Klunk W, et al. Research evaluation and prospective diagnosis of dementia with Lewy bodies. *Arch Neurol* 2002;59:43–6.
- McKeith IG, Ballard CG, Perry RH, Ince PG, O'Brien JT, Neill D, et al. Prospective validation of consensus criteria for the diagnosis of dementia with Lewy bodies. *Neurology* 2000;54:1050–8.
- Middlekoop HA, van der Flier WM, Burton EJ, Lloyd AJ, Paling S, Barber R, et al. Dementia with Lewy bodies and AD are not associated with occipital lobe atrophy on MRI. *Neurology* 2001;57:2117–20.
- Ishii K, Hosaka K, Mori T, Mori E. Comparison of FDG-PET and IMP-SPECT in patients with dementia with Lewy bodies. *Ann Nucl Med* 2004;18:447–51.
- Albin RL, Minoshima S, Damato CJ, Fley KA, Kuhl DA, Sima AAF. Fluoro-deoxyglucose positron emission tomography in diffuse Lewy body disease. *Neurology* 1996;47:462–6.
- Minoshima S, Foster NL, Sima AAF, Frey KA, Albin RL, Kuhl DE. Alzheimer's disease versus dementia with Lewy bodies: cerebral metabolic distinction with autopsy confirmation. *Ann Neurol* 2001;50:358–65.
- Lobotesis K, Fenwick JD, Phipps A, Ryman A, Swann A, Ballard C, et al. Occipital hypoperfusion on SPECT in dementia with Lewy bodies but not AD. *Neurology* 2001;56:643–9.
- Hansen L, Salmon D, Galasko D, Masliah E, Katzman R, De Teresa R, et al. The Lewy body variant of Alzheimer's disease: a pathological and clinical entity. *Neurology* 1990;40:1–8.
- Gerlach M, Stadler K, Aichner F, Ransmayr G. Dementia with Lewy bodies and AD are not associated with occipital lobe atrophy on MRI. *Neurology* 2002;59:1476.
- Ishii K, Willoch F, Minoshima S, Drzezga A, Ficaró EP, Cross DJ, et al. Statistical brain mapping of  $^{18}\text{F}$ -FDG PET in Alzheimer's

- disease: validation of anatomic standardization for atrophied brains. *J Nucl Med* 2001;42:548–57.
24. Marshall V, Grosset D. Role of dopamine transporter imaging in routine clinical practice. *Mov Disord* 2003;18:1415–23.
  25. Vaamonde-Gamo J, Flores-Barrangan JM, Ibanez R, Gudin M, Hernandez A. DaT-SCAN SPECT in the differential diagnosis of dementia with Lewy bodies and Alzheimer's disease. *Rev Neurol* 2005;41:276–9.
  26. Colloby SJ, O'Brien JT, Fenwick JD, Firbank ML, Burn DJ, McKeith IG, et al. The application of statistical parametric mapping to <sup>123</sup>I-FP-CIT SPECT in dementia with Lewy bodies, Alzheimer's disease and Parkinson's disease. *Neuroimage* 2004;23:956–66.
  27. Hu XS, Okamura N, Arai H, Higuchi M, Matsui T, Tashiro M, et al. <sup>18</sup>F-fluorodopa PET study of striatal dopamine uptake in the diagnosis of dementia with Lewy bodies. *Neurology* 2000;55:1575–7.